

Strained Bilayer Graphene, Emergent Energy Scales, and Moiré Gravity

Alireza Parhizkar¹ and Victor Galitski¹

¹*Joint Quantum Institute and Condensed Matter Theory Center,
University of Maryland, College Park, MD 20742, USA*

(Dated: May 3, 2022)

Twisted bilayer graphene is a rich condensed matter system, which allows one to tune energy scales and electronic correlations. The low-energy physics of the resulting moiré structure can be mathematically described in terms of a diffeomorphism in a continuum formulation. We stress that twisting is just one example of moiré diffeomorphisms. Another particularly simple and experimentally relevant transformation is a homogeneous isomorphic strain of one of the layers, which gives rise to a nearly identical moiré pattern (rotated by 90° relative to the twisted structure) and potentially flat bands. We further observe that low-energy physics of the strained bilayer graphene takes the form of a theory of fermions tunneling between two curved space-times. Conformal transformation of the metrics results in emergent “moiré energy scales,” which can be tuned to be much lower than those in the native theory. This observation generalizes to an arbitrary space-time dimension with or without an underlying lattice or periodicity and suggests a family of toy models of “moiré gravity” with low emergent energy scales. Motivated by these analogies, we present an explicit toy construction of moiré gravity, where the effective cosmological constant can be made arbitrarily small. We speculate about possible relevance of this scenario to the fundamental vacuum catastrophe in cosmology.

When two lattices overlap, they give rise to a moiré pattern as their emergent superlattice structure. The physical properties of such moiré superstructures have been extensively studied in the context of bilayer graphene [1–8]. The low-energy physics of graphene bilayers can be conveniently studied within a continuum model, where a general deformation is described by the two-dimensional diffeomorphism $\mathbf{x} \rightarrow \mathbf{x} + \boldsymbol{\xi}(\mathbf{x})$ where points at \mathbf{x} are translated by $\boldsymbol{\xi}$, which in general can be an arbitrary function of the position vector $\mathbf{x} \equiv (x, y)$. Starting with two layers with coinciding sites, deforming one of the layers by the flow $\boldsymbol{\xi}(\mathbf{x})$ yields a general bilayer superstructure. Specifically for the twisted bilayer graphene, the twist flow for small twist angles θ is given by $\boldsymbol{\xi}_t \equiv \theta \hat{z} \times \mathbf{x}$.

Much similar to this flow, but perpendicular to it is the flow due to a biaxial strain or uniform expansion of the layers. It is described by $\boldsymbol{\xi}_s \equiv \theta \mathbf{x}$, where we use the same notation θ for the expansion parameter. The strained and twisted vector fields are related to each other by a 90° rotation, $\boldsymbol{\xi}_t \cdot \boldsymbol{\xi}_s = 0$, as shown in Fig 1a. Furthermore, since the transformations are similar but orthogonal to each other, the corresponding emergent moiré patterns are also 90° rotated versions of each other. This is also shown in Fig. 1 where we have deformed one layer by $+\frac{\theta}{2}$ and the other layer by $-\frac{\theta}{2}$. Note that the combinatory effect of twist and different types of strain have been investigated both experimentally and theoretically in Refs. [9–14].

The main goal of the present Letter is to generalize this construction to a broad class of systems, by pointing out that moiré length and energy scales generally emerge in continuum theories, where two smooth manifolds of arbitrary dimension overlap or are coupled together, and where the metric of one of the manifolds is

a scaling diffeomorphism of the other. No underlying lattice structure, nor quantum mechanics are necessary for this purely geometric phenomenon to occur. However, since the appearance of large moiré patterns and small moiré bands in slightly strained bilayer graphene is worthy of explicit emphasis, and given the direct relevance to experiment, we first review the specific physics of uniformly strained bilayer graphene, with the main intention of following the geometric emergence of the small energy scales. Most results are straightforwardly transplanted from the case of twisted bilayer graphene, and so are discussed/reviewed in parallel.

The continuum model for both twisted and strained bilayer is given by the following Hamiltonian [15]

$$H_{t,s} = \int d^2x \left[\psi_+^\dagger h_{t,s}^{+\theta/2} \psi_+ + \psi_-^\dagger h_{t,s}^{-\theta/2} \psi_- + \psi_-^\dagger T_{t,s}(\boldsymbol{\xi}_{t,s}) \psi_+ + h.c. \right], \quad (1)$$

where ψ_\pm are fermionic operators, $L = \pm$ indexes the upper/lower layers, and $h_{t,s}^{\pm\theta/2} = -iv_F \boldsymbol{\sigma}_{t,s} \cdot \nabla$ is the single-particle Hamiltonian in layer $L = \pm$ deformed by $\pm\frac{\theta}{2}$ under the flow $\boldsymbol{\xi}_t$ or $\boldsymbol{\xi}_s$. Also v_F is the Fermi velocity and $\boldsymbol{\sigma}_{t,s}$ is $\boldsymbol{\sigma} = (\sigma^x, \sigma^y)$ transformed accordingly. Note that all the fields in the above equation depend on position. The inter-layer tunneling matrix T has two parts, a diagonal part proportional to σ^0 describing intra-sublattice (AA) tunneling and an off-diagonal part describing inter-sublattice (AB) tunneling. This results into two types of eigenvalues for the tunneling matrix, which overcome each other periodically over the moiré pattern. Therefore we expect the eigenvalues of the tunneling matrix for twisted and stretched bilayer to schematically follow Fig. 2.

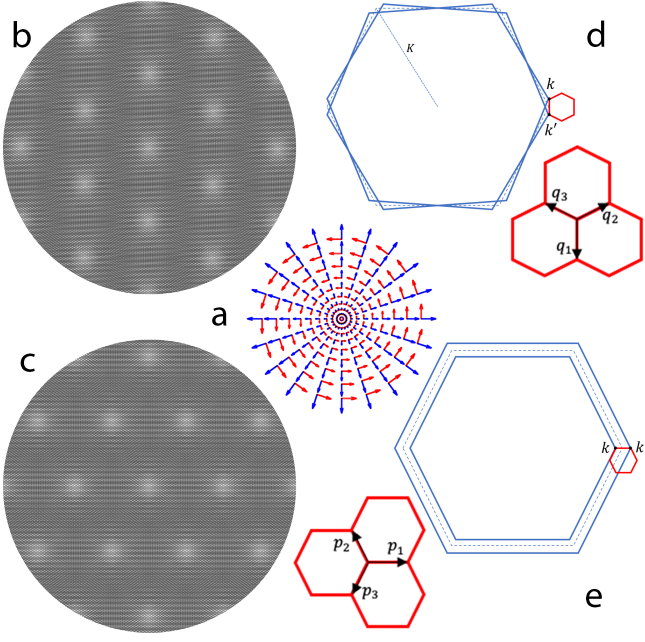


FIG. 1. (a) Generators of rotation and expansion drawn simultaneously: Blue arrows demonstrate the vector field ξ_s while red arrows demonstrate that of ξ_t . (b) and (c) are twisted and stretched bilayer graphene respectively. The parameters of both transformations are set to $\theta \approx 0.0192$. Moiré patterns of these bilayers are exactly the same but 90° rotated. Hexagonals (unit cells) of undeformed layers have their largest diameter along the vertical axis y . (d) and (e) schematically show Brillouin zones of twisted and stretched bilayer respectively (blue hexagonals); both give rise to their corresponding moiré reciprocal lattices (red hexagonals)

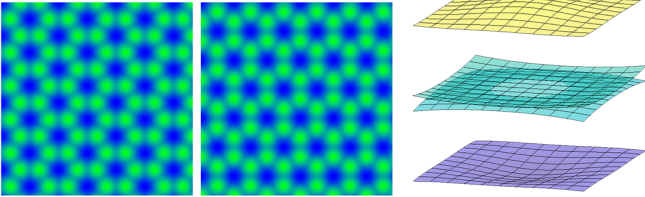


FIG. 2. From left to right: Tunneling matrix for twisted bilayer - Tunneling matrix for stretched bilayer - Vanishing of the renormalized Fermi velocity at K valley for magic scale $\theta \approx 0.0192$. Green designates regions where AB tunnelings are dominant and blue shows that of AA tunnelings.

The tunneling matrix T_t for twisted bilayer graphene in real space is given by $T_t(\mathbf{x}) = \sum_j e^{-i\mathbf{q}_j \cdot \mathbf{x}} T_j^t$ with $\mathbf{q}_1 = k_\theta(0, -1)$, $\mathbf{q}_{2,3} = k_\theta(\pm\sqrt{3}/2, 1/2)$ and [15, 16]

$$T_j^t = u \begin{pmatrix} 1 & 0 \\ 0 & 1 \end{pmatrix} + w \begin{pmatrix} 0 & e^{-i\frac{2\pi}{3}(j-1)} \\ e^{i\frac{2\pi}{3}(j-1)} & 0 \end{pmatrix}, \quad (2)$$

where u and w are respectively AA and AB inter-layer coupling parameters and $k_\theta \equiv K\theta = \frac{4\pi}{3\sqrt{3}a}\theta$. Since T_s is a 90° rotated version of T_t then one expects

$T_s(\mathbf{x}) = \sum_j e^{-i\mathbf{p}_j \cdot \mathbf{x}} T_j^s$ with $\mathbf{p}_1 = k_\theta(1, 0)$ and $\mathbf{p}_{2,3} = k_\theta(-1/2, \pm\sqrt{3}/2)$.

The Brillouin zone of a single layer of graphene is hexagonal with two valleys K and K' where Dirac cones reside. A transformation of a single layer in real space, transforms the reciprocal lattice accordingly. In the twisted bilayer, when one layer is rotated by $+\frac{\theta}{2}$ and the other by $-\frac{\theta}{2}$, the corresponding reciprocal lattices of the two single layers also rotate by the same angles. This is due to the fact that rotation applies to all vectors; therefore it will also take place in the momentum space where $\mathbf{k} \equiv (k_x, k_y)$ has rotated in the same way as \mathbf{x} . If we concentrate only on one valley, say K, then we see that rotation separates the K valleys of the two layers by k_θ as shown in Fig. 1d.

The same happens for the uniformly strained bilayer. The single layer, stretched by $+\frac{\theta}{2}$ in real space, experiences a shrinkage in momentum space by the same factor, and the inverse effect happens to the other layer. Since, like the above case of twisted bilayer, we have respected all the symmetries of graphene through this deformation, the hexagonal structure is preserved. Therefore, a moiré reciprocal pattern emerges similar to twisted bilayer but rotated by 90 degrees, see Fig 1e.

By looking at the moiré reciprocal lattices of the both bilayers, figures 1d and 1e, we see that there are three different paths an electron can take while tunneling between layers from k to k' . The three-momentum vectors $\{\mathbf{p}_1, \mathbf{p}_2, \mathbf{p}_3\}$ in strained bilayer are the 90° counterclockwise rotated version of $\{\mathbf{q}_1, \mathbf{q}_2, \mathbf{q}_3\}$ in twisted bilayer. An electron at the end of \mathbf{p}_1 compared to an electron at the end of \mathbf{q}_1 is rotated by 90° or by $e^{i\frac{\pi}{4}\sigma^z}$. If T_s is indeed related to T_t by a rotation then we should be able to write

$$T_s(\xi_s) = e^{-i\frac{\Omega}{2}\sigma^z} T_t(R(\Omega)\xi_t) e^{i\frac{\Omega}{2}\sigma^z}, \quad \Omega = \frac{\pi}{2}, \quad (3)$$

where both spinor degrees of freedom of T_t and its argument are rotated by 90° . Then one can numerically [17] and analytically [16] (for the chiral limit where $u = 0$) show that there are magic scales θ where the band structure of the stretched bilayer develops a flat band; see Fig. 2. Note however that if the tunneling matrix does not satisfy condition (3), flat bands would not necessarily appear.

Now, we rewrite the Hamiltonian for a bilayer deformed by an arbitrary flow $\xi_\pm(\mathbf{x})$ in the following geometric form

$$H = \int d^2x \left[\psi_+^\dagger e_{l_+}^\mu \sigma^l D_\mu^+ \psi_+ + \psi_-^\dagger e_{l_-}^\mu \sigma^l D_\mu^- \psi_- + \psi_-^\dagger T_\xi (\xi_+(\mathbf{x}) - \xi_-(\mathbf{x})) \psi_+ + h.c. \right], \quad (4)$$

where $D_\mu^\pm = \partial_\mu + \mathcal{A}_l^\pm e_{l_\pm}^\mu$ with $e_{l_\pm}^\mu = \delta_l^\mu + \frac{\partial \xi_\pm^\mu}{\partial x^l}$ being the vielbeins of the two-dimensional space of each single

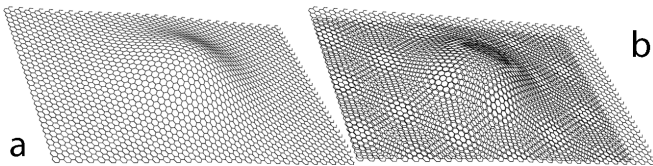


FIG. 3. (a) A single curved layer of graphene. (b) A bilayer constructed from two equally curved layers with unequal graphene charts. One chart is slightly shrunken relative to the other which has resulted in the familiar moiré patterns.

layer deformed by ξ_{\pm} and \mathcal{A}_l^{\pm} gauge fields induced by the flow (e.g. non-uniform strain) [18, 19] in each layer. Explicitly, for a single layer, \mathcal{A}_l is defined as

$$\mathcal{A}_l = \frac{\gamma}{a} \begin{pmatrix} \partial_x \xi_x - \partial_y \xi_y \\ \partial_x \xi_y + \partial_y \xi_x \end{pmatrix}, \quad \gamma \equiv \frac{\partial \ln t}{\partial \ln a} \quad (5)$$

where t is the hopping strength. So far the geometry of each single layer has been considered to be flat. However, due to the robustness of the Dirac points we can still include slight deviations from the flatness to our considerations as well. We can imagine a curved layer of graphene as a curved surface covered by a hexagonal chart of graphene. The diffeomorphism flow, ξ , transforms the chart to another leaving the surface untouched. To consider a curved bilayer, therefore, we use two relatively transformed curved vielbeins $e_{l\pm}^{\mu} = e_l^{\mu} + \frac{\partial \xi_{\pm}^{\mu}}{\partial x^l}$ with the original curved vielbein e_l^{μ} yielding the induced metric $h^{\mu\nu}$ on the surface through $h^{\mu\nu} = e_m^{\mu} e_n^{\nu} \delta^{mn}$ where δ^{mn} is the metric of the flat space. If we describe the two dimensional curved surface as a membrane embedded in a three dimensional flat manifold, Fig. 3, whose points satisfy the relation $z = h(x, y)$ with z being the extra dimension, then the induced metric $h_{\mu\nu}$ on this surface is given by,

$$h_{\mu\nu} dx^{\mu} dx^{\nu} = (1 + (\partial_x h)^2) dx^2 + 2\partial_x h \partial_y h dx dy + (1 + (\partial_y h)^2) dy^2. \quad (6)$$

Because of the curvature, π -orbitals which were aligned before will now make a locally varying angle with each other and consequently result in a locally varying hopping parameter which ultimately gives rise to an additional gauge field \mathcal{A}_l^c appearing in the same way as \mathcal{A}_l inside the covariant derivative. For small $h(x, y)$ it is given by

$$\mathcal{A}_l^c = \epsilon_{\pi\pi} \frac{3a^2}{8} \begin{pmatrix} (\partial_y^2 h)^2 - (\partial_x^2 h)^2 \\ 2\partial_x \partial_y h (\partial_x^2 h + \partial_y^2 h) \end{pmatrix}, \quad (7)$$

with $\epsilon_{\pi\pi} = 2.89\text{eV}$ for graphene.[18, 20] Note that one can also attribute unequal curvatures to the layers by considering them having unequal induced metrics. In that case the difference in curvature itself will automatically introduce a moiré pattern.

Parallel transportation of fermions on a curved space-time is determined by the covariant Dirac operator $\mathcal{D} \equiv e_k^{\mu} \sigma^k (\partial_{\mu} + A_{\mu}^{mn} [\sigma_m, \sigma_n])$. However, using the algebra of Pauli matrices and disregarding time components we can write this Dirac operator as $\mathcal{D} = e_k^{\mu} \sigma^k (\partial_{\mu} + \mathcal{A}_l e_{\mu}^l)$ with \mathcal{A}_l defined as $\mathcal{A}^l \equiv e_m^{\mu} A_{\mu}^{[ml]}$. Therefore, written in the above form (4), the bilayer problem resembles a fermionic field theory where the electron is allowed to tunnel between two different “universes” with their designated geometries given by the metrics $g_{\pm}^{\mu\nu} = e_{m\pm}^{\mu} e_{n\pm}^{\nu} \eta^{mn}$. Here η^{mn} is the flat metric. The interlayer tunneling plays the role of a “wormhole” process in this formulation.[21]

This perspective allows us to identify minimal “ingredients” needed for moiré physics, which we define as the emergence of new energy/length scales in two superimposed systems, much smaller/larger compared to the corresponding scales in the individual systems. We observe that no underlying lattice is necessary, and two continuum models (even with a random structure) may give rise to similar phenomena. We further notice that these conclusions are independent of dimensionality. These general considerations motivate us to broaden the scope of physical models, where these scenarios can be explored, beyond canonical condensed matter systems. A class of models where the moiré scenario may be of potential interest is general relativity/cosmology, in particular the cosmological constant problem. Below we propose a toy model where superimposing “universes” with large individual cosmological constants gives rise to an arbitrarily small effective cosmological constant.

The problem with the cosmological constant Λ can be stated in multiple ways (for a review, see e.g. Refs. [22] and [23]). One of which is to ask: How can one naturally get a small or zero value for the gravitating cosmological constant, while the scales of the theory are huge in comparison? All the fields in the Standard Model contribute to the zero-point energy density. Because gravity couples to all forms of energy, the gravitational effects of the zero-point energy must in general be observable. But this is not consistent with observations, which show the energy density much smaller than all other scales in the Standard Model. On the other hand, the history of the universe and the resulting cosmology can be very sensitive to a model chosen to describe the vacuum energy. Trying to reconcile all these with observations leads to a fine tuning problem. In the light of such problems then, the possibility of an emergent small scale might be a question of interest. What follows is a simple model inspired by the moiré physics, which can investigate this possibility. Note that the toy model of “moiré gravity” below is not unique and other similar setups can be constructed with different mechanism of overlapping geometries.

The classical theory of general relativity in the presence of matter fields is given by the following action de-

vised for the Neumann boundary conditions,

$$S_c = \int d^4x \sqrt{-g} \left[\frac{c^4}{8\pi G} (R - 2\Lambda) + \mathcal{L}(\phi) \right], \quad (8)$$

where g is the determinant of the metric $g_{\mu\nu}$, $\mathcal{L}(\phi)$ is the Lagrangian of all other fields in the theory, $c = 1$ is the speed of light and $G = M_P^{-2}$ is the constant of gravitation with M_P being the Planck mass. The largest scales of the theory are set by M_P . In four dimensional spacetime, then, a dimensionless action is provided only if Λ scales with mass squared which sets the conjectured value of $\pm M_P^2$ for the cosmological constant. A more careful QFT consideration of the zero-point energy also casts the same guess. It is important to note that although it is to some extent meaningful to decide about the magnitude of a variable such as Λ by the scales of the theory, one cannot decide about the sign of that variable using only the scales. Nonetheless, $+M_P^2$ and $-M_P^2$ are way larger than what the cosmological constant is observed to be.

The Planck mass also roughly represents the upper bound for energy scales of measurement, or inversely, how accurately we can measure length. As we approach the limit of M_P^{-1} the theory is expected to break down and, quite similar to condensed matter systems, a microstructure should reveal itself when the wavelengths of intended observations are no longer blind to the underlying structure. Therefore, if spacetime was a lattice, the distance between the sites would have roughly been M_P^{-1} . This incites the idea that a combination of two such structures with slightly different length scales, can give rise to another moiré length scale much longer than the two.

Then let us consider two copies of the classical theory with different metrics, which one can picture as two copies of a universe with the combined following action,

$$\begin{aligned} S_g + S_h &= \int d^4x \sqrt{-g} \left[\frac{c^4}{8\pi G} (R_g - 2\Lambda_g) + \mathcal{L}_g(\phi) \right] \\ &+ \int d^4x \sqrt{-h} \left[\frac{c^4}{8\pi G} (R_h - 2\Lambda_h) + \mathcal{L}_h(\phi) \right], \end{aligned} \quad (9)$$

where $g_{\mu\nu}$ and $h_{\mu\nu}$ are the metrics of the two universes. Here S_g and S_h are already coupled through matter fields ϕ , but for the present let us forget about non-geometrical fields and instead introduce an inter-universe coupling via a purely geometrical coupling term

$$S_{gh} = \frac{c^4}{2\pi G} \int d^4x \sqrt{|g, h|} \bar{\Lambda}, \quad (10)$$

where $|g, h|$ is generically any term built out of metrics $h_{\mu\nu}$ and $g_{\mu\nu}$. In what follows we set $\frac{c^4}{8\pi G} = 1$ and define $|g, h|$ to resemble g and h as below

$$|g, h| \equiv \frac{1}{4!} \varepsilon^{\mu\nu\alpha\beta} \varepsilon^{\rho\sigma\lambda\gamma} g_{\mu\rho} g_{\nu\sigma} h_{\alpha\lambda} h_{\beta\gamma}, \quad (11)$$

where $\varepsilon^{\mu\nu\alpha\beta}$ is the Levi-Civita symbol. The crossbred determinant (11) transforms akin to metric determinant $g \equiv \frac{1}{4!} \varepsilon^{\mu\nu\alpha\beta} \varepsilon^{\rho\sigma\lambda\gamma} g_{\mu\rho} g_{\nu\sigma} g_{\alpha\lambda} g_{\beta\gamma}$ under general coordinate transformations. So, the two universes are coupled through a shared or mixed volume element. Note that there is no ambiguity in lowering and raising indices. The metric $g_{\mu\nu}$ is responsible for that of objects belonging to g -universe and the same goes for $h_{\mu\nu}$ and h -universe. For conformally flat metrics, which suffice for our present purposes, $|g, h|$ becomes equivalent to $\sqrt[4]{g\bar{h}}$. We have adopted the former here merely to point out a wider range of possibilities. However, looking back at the Hamiltonian (4), we can think of the spinor degrees of freedom as fermionic fields that each have absorbed half a corresponding vielbein determinant $\psi_{\pm} \equiv \sqrt{|e_{\pm}|} \hat{\psi}_{\pm}$, while each vielbein determinant $|e_{\pm}|$ is itself equivalent to the square root of its corresponding metric determinant. In fact, the quantum variables, for example in path-integral formulation of fermions on curved background, must be of this type if the theory is to be diffeomorphism invariant. This establishes a common characteristic between inter-layer and inter-universe tunnelings. A conformal transformation of only one metric transforms the coupling term halfway through.

To obtain the equations of motion we vary the action $S = S_g + S_h + S_{gh}$ with respect to the inverse metrics $g^{\mu\nu}$ and $h^{\mu\nu}$. Since the action is symmetric under $g \leftrightarrow h$ we are only going to write one set of these equations in what follows unless required otherwise. Variation of S_g and S_h gives the usual Einstein tensor with their corresponding cosmological constants, and the variation of the coupling term is obtained by looking at (11) and noticing $\delta g^{\mu\nu} = -g^{\mu\alpha} g^{\nu\beta} \delta g_{\alpha\beta}$. The result is

$$\begin{aligned} \sqrt{-g} \left(R_{\mu\nu}^g - \frac{1}{2} R^g g_{\mu\nu} + \Lambda_g g_{\mu\nu} \right) &= \\ \frac{\bar{\Lambda}}{3!} |g, h|^{-\frac{1}{2}} \varepsilon^{\kappa\zeta\alpha\beta} \varepsilon^{\rho\sigma\lambda\gamma} g_{\mu\kappa} g_{\nu\rho} g_{\zeta\sigma} h_{\alpha\lambda} h_{\beta\gamma}. \end{aligned} \quad (12)$$

Let us now settle to a class of solutions which enjoy a large amount of symmetry, by choosing the Friedmann–Lemaître–Robertson–Walker metric with a conformal time t ,

$$ds_g^2 = a_g^2(t) \eta_{\mu\nu} dx^\mu dx^\nu \equiv g_{\mu\nu} dx^\mu dx^\nu \quad (13)$$

$$ds_h^2 = a_h^2(t) \eta_{\mu\nu} dx^\mu dx^\nu \equiv h_{\mu\nu} dx^\mu dx^\nu, \quad (14)$$

Note that even though the coupling action S_{gh} is invariant under coordinate transformations, choosing both metrics to have the above form is a kinetic restriction since, for example, there are no coordinate transformations that can generally transform both metrics to have the form $ds^2 = -dt^2 + a^2(t) d\mathbf{x}^2$. But we deliberately restrict ourselves to this class of double-metrics since they present the simplest pathway for our model. So, we arrive at two sets of equations. From (12) for $\mu = \nu = 0$

we have

$$3\dot{a}_g^2 - \Lambda_g a_g^4 - \bar{\Lambda} a_g^2 a_h^2 = 0 \quad (15)$$

and for $\mu = \nu = \{1, 2, 3\}$,

$$\dot{a}_g^2 - 2\ddot{a}_g a_g + \Lambda_g a_g^4 + \bar{\Lambda} a_g^2 a_h^2 = 0. \quad (16)$$

The solutions are

$$a_g = \frac{A_g}{t + \tau_g} \text{ and } a_h = \frac{A_h}{t + \tau_h}, \quad (17)$$

with $A_{h,g}$ and $\tau_{h,g}$ being the constants of integration. A solution to the above equations does not always exist, but requires the consistency relation between Λ s to be satisfied. If we let Λ s depend on time it is given by

$$\Lambda_g = \Lambda_{\text{eff}}^g - \frac{\Lambda_{\text{eff}}^g}{\Lambda_{\text{eff}}^h} \left(\frac{t + \tau_g}{t + \tau_h} \right)^2 \bar{\Lambda}, \quad (18)$$

where Λ_{eff}^g and Λ_{eff}^h are respectively defined as $3/A_g^2$ and $3/A_h^2$ and they appear in the equations of motion as

$$3\dot{a}_g^2 - \Lambda_{\text{eff}}^g a_g^4 = 0 \quad (19)$$

$$\dot{a}_g^2 - 2\ddot{a}_g a_g + \Lambda_{\text{eff}}^g a_g^4 = 0. \quad (20)$$

The above consistency relations mean that there exists a solution *if and only if*

$$\bar{\Lambda} a_g^2 a_h^2 + \Lambda_g a_g^4 = \Lambda_{\text{eff}}^g a_g^4, \quad (21)$$

where Λ_{eff}^g is a constant. If we choose $\Lambda_{\text{eff}}^g = \Lambda_{\text{eff}}^h \equiv \Lambda_{\text{eff}}$ then by combining the two consistency relations we have,

$$\Lambda_{\text{eff}} = \frac{\Lambda_g a_g^4 - \Lambda_h a_h^4}{a_g^4 - a_h^4} = \frac{\Lambda_g \nu_g - \Lambda_h \nu_h}{\nu_g - \nu_h}, \quad (22)$$

where the moiré relation is more clarified, with $\nu_{g,h}$ being spacetime volume elements of each universe in a global coordinate system.

The magnitudes of Λ_h , Λ_g and $\bar{\Lambda}$, which directly appear in the action, are set by the scale of the theory to be either of order M_P^2 or zero. But Λ_{eff} depends only on the constants of integration and therefore is arbitrarily chosen, which can be set to a very small value. For example, set $\Lambda_{\text{eff}}^g = \Lambda_{\text{eff}}^h \ll 1$, $\bar{\Lambda} = -M_P^2$ and $\tau_h = \tau_g + \Delta\tau$. Then although at first Λ_h and Λ_g differ, they approach equality at long enough times.

We can also take the opposite path. Let us choose the $\Lambda_{\text{eff}}^g = \Lambda_{\text{eff}}^h = \bar{\Lambda} = M_P^2$ and $\tau_h = \tau_g + \Delta\tau$, with $\Delta\tau \gg 1$,

$$\Lambda_{g,h} = M_P^2 \left[1 - \left(\frac{t + \tau_{g,h}}{t + \tau_{h,g}} \right)^2 \right]. \quad (23)$$

Then we get two universes that start way out of equilibrium with sizable cosmological constants, one negative and one positive, and gradually approach equilibrium at which their isolated cosmological constants vanish.

This work originated from a project supported by the Templeton Foundation. This research was also supported by the Simons Foundation.

-
- [1] Yuan Cao, Valla Fatemi, Ahmet Demir, Shiang Fang, Spencer L Tomarken, Jason Y Luo, Javier D Sanchez-Yamagishi, Kenji Watanabe, Takashi Taniguchi, Efthimios Kaxiras, *et al.*, ‘‘Correlated insulator behaviour at half-filling in magic-angle graphene superlattices,’’ *Nature* **556**, 80–84 (2018).
 - [2] Yuan Cao, Valla Fatemi, Shiang Fang, Kenji Watanabe, Takashi Taniguchi, Efthimios Kaxiras, and Pablo Jarillo-Herrero, ‘‘Unconventional superconductivity in magic-angle graphene superlattices,’’ *Nature* **556**, 43–50 (2018).
 - [3] J. M. B. Lopes dos Santos, N. M. R. Peres, and A. H. Castro Neto, ‘‘Graphene bilayer with a twist: Electronic structure,’’ *Phys. Rev. Lett.* **99**, 256802 (2007).
 - [4] Eva Y Andrei and Allan H MacDonald, ‘‘Graphene bilayers with a twist,’’ *Nature materials* **19**, 1265–1275 (2020).
 - [5] Amol Nimbalkar and Hyunmin Kim, ‘‘Opportunities and challenges in twisted bilayer graphene: a review,’’ *Nano-Micro Letters* **12**, 1–20 (2020).
 - [6] A. O. Sboychakov, A. L. Rakhmanov, A. V. Rozhkov, and Franco Nori, ‘‘Electronic spectrum of twisted bilayer graphene,’’ *Phys. Rev. B* **92**, 075402 (2015).
 - [7] Liujun Zou, Hoi Chun Po, Ashvin Vishwanath, and T. Senthil, ‘‘Band structure of twisted bilayer graphene: Emergent symmetries, commensurate approximants, and wannier obstructions,’’ *Phys. Rev. B* **98**, 085435 (2018).
 - [8] M Van der Donck, C De Beule, B Partoens, F M Peeters, and B Van Duppen, ‘‘Piezoelectricity in asymmetrically strained bilayer graphene,’’ *2D Materials* **3**, 035015 (2016).
 - [9] Nathanael P Kazmierczak, Madeline Van Winkle, Colin Ophus, Karen C Bustillo, Stephen Carr, Hamish G Brown, Jim Ciston, Takashi Taniguchi, Kenji Watanabe, and D Kwabena Bediako, ‘‘Strain fields in twisted bilayer graphene,’’ *Nature Materials*, 1–8 (2021).
 - [10] Wei Yan, Wen-Yu He, Zhao-Dong Chu, Mengxi Liu, Lan Meng, Rui-Fen Dou, Yanfeng Zhang, Zhongfan Liu, Jia-Cai Nie, and Lin He, ‘‘Strain and curvature induced evolution of electronic band structures in twisted graphene bilayer,’’ *Nature communications* **4**, 1–7 (2013).
 - [11] Zhen Bi, Noah F. Q. Yuan, and Liang Fu, ‘‘Designing flat bands by strain,’’ *Phys. Rev. B* **100**, 035448 (2019).
 - [12] Marcin Mucha-Kruczyński, Igor L. Aleiner, and Vladimir I. Fal’ko, ‘‘Strained bilayer graphene: Band structure topology and landau level spectrum,’’ *Phys. Rev. B* **84**, 041404 (2011).
 - [13] Marwa Mannai and Sonia Haddad, ‘‘Twistronics versus straintronics in twisted bilayers of graphene and transition metal dichalcogenides,’’ *Phys. Rev. B* **103**, L201112 (2021).
 - [14] Jen-Hsien Wong, Bi-Ru Wu, and Ming-Fa Lin, ‘‘Strain effect on the electronic properties of single layer and bilayer graphene,’’ *The Journal of Physical Chemistry C* **116**, 8271–8277 (2012), <https://doi.org/10.1021/jp300840k>.
 - [15] Leon Balents, ‘‘General continuum model for twisted bilayer graphene and arbitrary smooth deformations,’’ *Sci-*

- Post Phys. **7**, 48 (2019).
- [16] Grigory Tarnopolsky, Alex Jura Kruchkov, and Ashvin Vishwanath, “Origin of magic angles in twisted bilayer graphene,” *Phys. Rev. Lett.* **122**, 106405 (2019).
- [17] Rafi Bistritzer and Allan H. MacDonald, “Moiré bands in twisted double-layer graphene,” *Proceedings of the National Academy of Sciences* **108**, 12233–12237 (2011), <https://www.pnas.org/content/108/30/12233.full.pdf>.
- [18] A. H. Castro Neto, F. Guinea, N. M. R. Peres, K. S. Novoselov, and A. K. Geim, “The electronic properties of graphene,” *Rev. Mod. Phys.* **81**, 109–162 (2009).
- [19] Hidekatsu Suzuura and Tsuneya Ando, “Phonons and electron-phonon scattering in carbon nanotubes,” *Phys. Rev. B* **65**, 235412 (2002).
- [20] Eun-Ah Kim and A. H. Castro Neto, “Graphene as an electronic membrane,” *EPL (Europhysics Letters)* **84**, 57007 (2008).
- [21] Of course, by this we do not mean the formation of an Einstein-Rosen bridge. Metric is not a dynamical field in (4), instead one can imagine a potential barrier between the layers that fermions are allowed to pass through by the tunneling process.
- [22] CP Burgess, “The cosmological constant problem: why it’s hard to get dark energy from micro-physics,” *Post-Planck Cosmology*, 149–197 (2013).
- [23] Antonio Padilla, “Lectures on the cosmological constant problem,” arXiv preprint arXiv:1502.05296 (2015).